Combita Merchán, DF.; Concepción Heydorn, P.; Corma Canós, A. (2014). Gold catalysts for the synthesis of aromatic azocompounds from nitroaromatics in one step. Journal of Catalysis. 311:339-349. doi:10.1016/j.jcat.2013.12.014.

GOLD CATALYSTS FOR THE SYNTHESIS OF AROMATIC AZOCOMPOUNDS FROM NITROAROMATICS IN ONE STEP

D. Combita, P. Concepción, A. Corma*

Instituto de Tecnología Quimica (UPV-CSIC)

Avenida de los Naranjos s/n 46022 Valencia (Spain)

acorma@itq.upv.es

ABSTRACT

One step selective hydrogenation of nitroaromatics to obtain symmetric azocompounds with high yields has been performed with a gold supported on cerium oxide catalysts. Au/TiO_2 and Au/CeO_2 catalysts direct the reaction by two different pathways and with different selectivities. In situ FTIR studies reveal that the surface concentration of the intermediate nitrosobenzene is decisive in directing the reaction trough the different reaction pathways. In this way, while on Au/TiO_2 a fast hydrogenation of the nitrosobenzene intermediate leads to a low surface concentration of the nitrosocompound, on Au/CeO_2 nitrosobenzene is more stabilized on the catalyst surface leading to a lower hydrogenation and a higher coupling rate, resulting in high selectivities to azobenzene. On Au/CeO_2 the relative weak adsorption of the azo with respect to the azoxycompound on the catalyst surface, avoids the consecutive hydrogenation of azocompounds to the corresponding anilines until all the azoxy has been consumed. Asymmetric azobenzenes have also been obtained with very high yields on TiO_2, through the Mills reaction.

INTRODUCTION

Aromatic azocompounds are widely used[1] as dyes[2], food additives[3] and drugs[4]. A major industrial process for their synthesis involves the azocoupling reaction between a diazonium salt and an activated arene[5]. The diazonium salt is prepared *in situ*, oxidizing an aromatic amine with sodium nitrite and a strong acid[6]. Other processes involve the oxidation of anilines to nitrosocompounds which furthermore react with aromatic amines in glacial acetic acid (Mills reaction)[7], or the rearrangement of an aromatic azoxycompound, obtained by nitrocompounds reduction using concentrated acids (Wallach reaction)[8](see scheme 1). Even if all these processes are quite effective, they involve several steps and generate a considerable amount of by-products.

a)

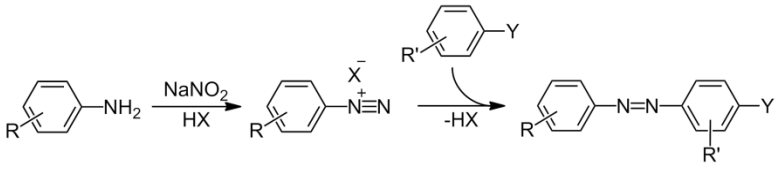

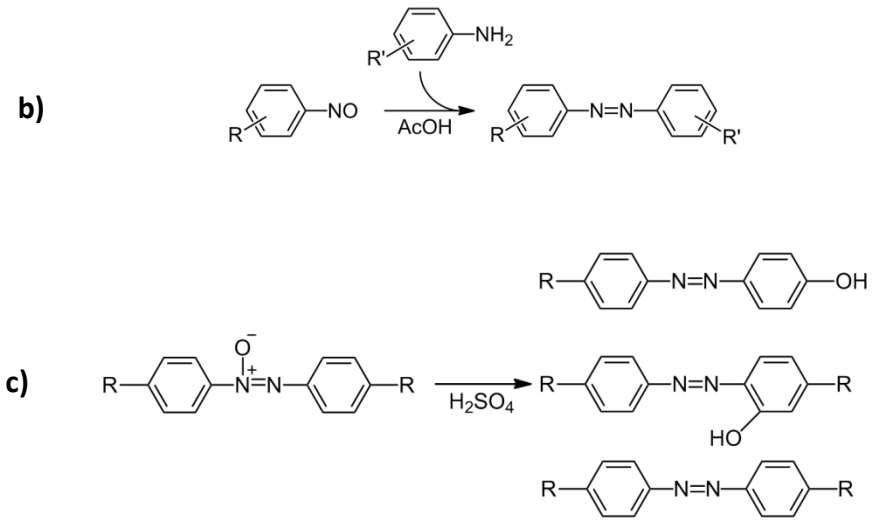

Scheme 1. Azocompounds synthesis: a) Azocoupling reaction; b) Mills Reaction and c) Wallach reaction.

An alternative for the synthesis of symmetric azocompounds is the reductive coupling of aromatic nitrocompounds using different types of reductive agents[9]. However, this process also generates a large amount of by-products implying intensive post-treatments. There is, therefore a great interest to develop catalytic heterogeneous methods to directly produce azocompounds from aromatic nitrocompounds.

Along these lines, we recently reported a two stage waste-free process catalyzed by Au/TiO_2 to obtain symmetric and asymmetric azocompounds starting from nitrobenzene and substituted nitrobenzenes, reaching high conversion and selectivity to the azocompounds[10]. Later, Zhu *et al*. using a photocatalytic reaction with Au/ZrO_2 as catalyst, in alkaline media (KOH) and room temperature, have reported high nitrocompounds conversions with moderate to good yields to symmetric azocompounds[11]. However it should be noticed that the ratio of solvent to reactant in this process is 392/3 mmol. Similarly, Hu *et al*. have prepared Pt and Pd nanowire catalysts to obtain, in the presence of KOH, symmetric and asymmetric azocompounds with moderate to good yields[12]. Very recently selectivities to azocompounds close to 15% have been achieved with supported gold catalysts pointing to the importance of the support on the final selectivity[13].

If one considers the general reaction scheme proposed by Haber[14] to reduce nitroaromatics (see Scheme 2), it should be possible to prepare azocompounds from nitrobenzenes in a single pass via the corresponding azoxycompounds, provided that a catalyst could be found which is able to direct the reaction via the intermediate nitrosocompound and aromatic hydroxylamine (routes a.1 and a.2 in Scheme 2) and to avoid the total hydrogenation to aniline. It should also be possible to produce azocompounds by reacting the intermediate nitrosocompound with aniline (see route b in Scheme 2). This last route would require a relatively slower reduction of

nitrosocompound to aniline, and a very fast reaction between nitrosobenzene and aniline.

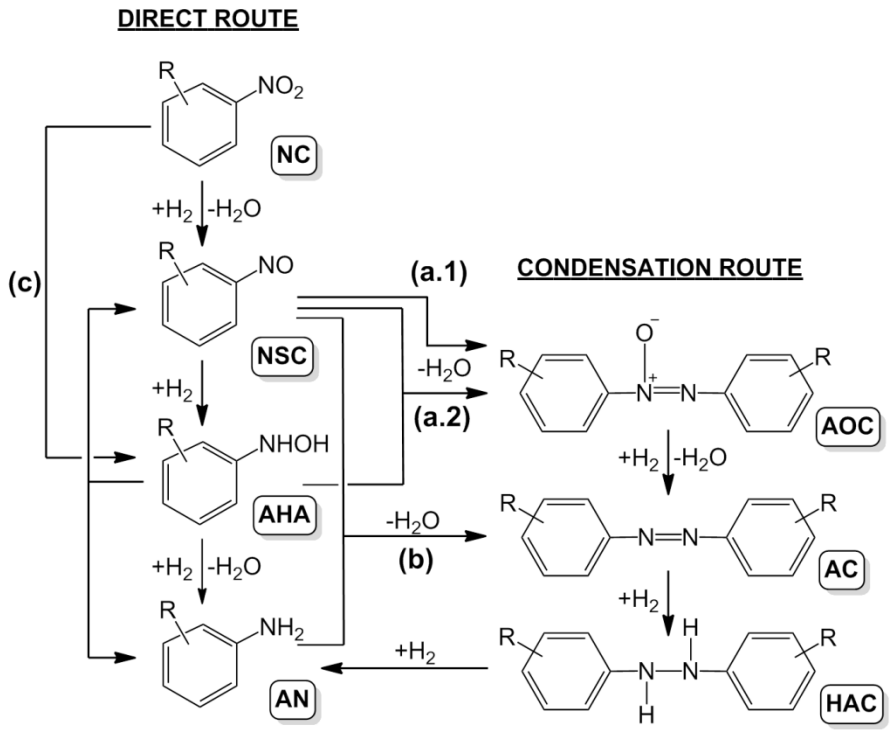

Scheme 2. Reaction pathways for the hydrogenation of nitrocompounds to anilines. NC: nitrocompound, NSC: nitrosocompound, AHA: aromatic hydroxylamine, AN: aniline, AOC: azoxycompound, AC: azocompound, HAC: hydrazocompound. Adapted from Richner *et al*.[15]

In the present work we show that it is possible to produce azocompounds with more than 98% yield from nitrobenzene in a single pass with a catalyst able to preferentially direct the process towards the coupling of nitrosobenzene intermediate (condensation route a.1 in Scheme 2). In this way the azoxycompound is formed that selectively evolves to the desired azocompound. This is achieved with gold on nanoparticulated CeO_2 in where the subsequent hydrogenation of the azocompound to produce aniline is inhibited. With this catalyst it is possible to reach very high conversion and selectivity while with Au/TiO_2 the full hydrogenation to aniline is favoured and the azocompound is not formed.

In the second part of the work we will present that while Au/CeO_2 is not a selective catalyst to produce asymmetric azocompounds, TiO_2 is a selective catalyst to perform the coupling between nitrosocompounds and anilines, yielding asymmetric azocompounds with high selectivities.

RESULTS AND DISCUSSION

Figure 1 presents the kinetic curves for the hydrogenation of nitrobenzene with Au/TiO_2 (a) and Au/CeO_2 (b). It can be seen there that over Au/TiO_2 the nitrobenzene converts almost exclusively to aniline, with small amounts of azobenzene being observed at the end of the reaction. However, when Au/CeO_2 was used as catalyst, the reaction follows the condensation route to form azoxybenzene and azobenzene. This implies that, according to the reaction pathways in Scheme 2, Au/CeO_2 should catalyze the condensation route between two nitrosobenzene molecules or between nitrosobenzene and hydroxylamine (routes a.1 and a.2). Though those intermediates were not detected in the liquid phase during the reaction, they must be present on the surface of the catalyst and the reaction between these two reactants on the catalyst surface should be very fast.

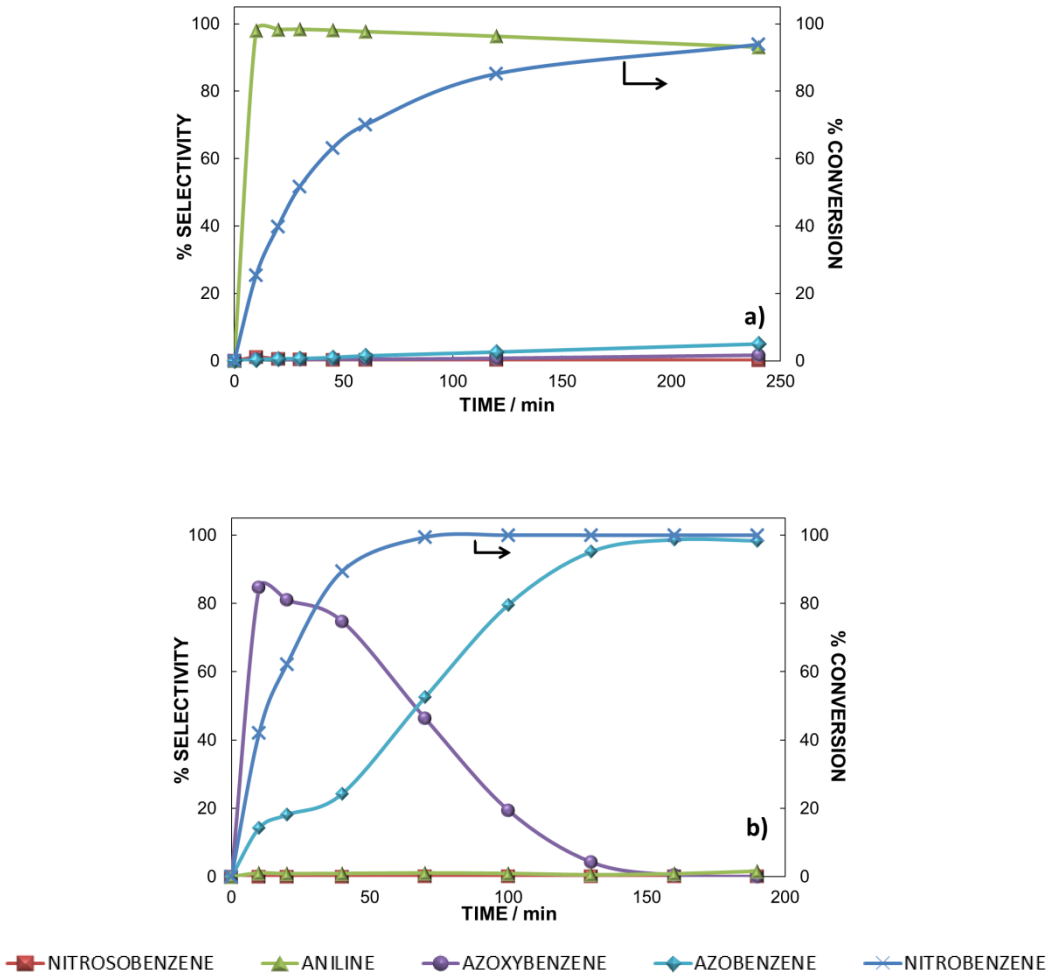

Figure 1. Nitrobenzene reaction profile over (a) Au/TiO_2, 1.5%wt Au and (b) Au/CeO_2, 1.5%wt Au. [Nitrobenzene]= 0.25M in toluene; Au= 1% mol; T= 120 ºC; P_0= 4 bar H_2.

Nevertheless, the most remarkable observation is that the Au/TiO_2 is a very active and selective catalyst to form aniline, while in the case of Au on nanoparticulated CeO_2 aniline is only observed when all nitrobenzene and azoxybenzene have reacted. From the above results one could think, in a first approximation, that the reaction follows

different routes with Au/TiO_2 and Au/CeO_2. If this was so, then Au/TiO_2 would preferentially catalyze the route given in Scheme 3, while Au/CeO_2 should catalyze the alternative route given in Scheme 4.

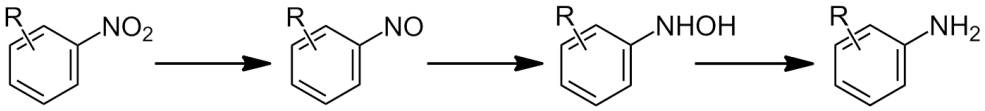

Scheme 3. Pathway followed by the Au/TiO_2 catalyzed hydrogenation of nitrocompounds.

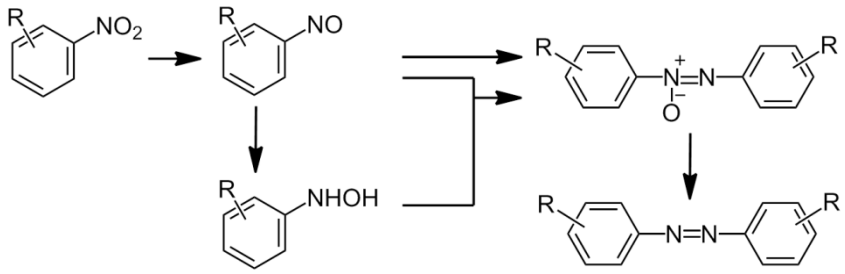

Scheme 4. Pathway followed by the Au/CeO_2 catalyzed hydrogenation of nitrocompounds.

There is another possibility to explain the high selectivity of Au/TiO_2 to aniline, by assuming that the reaction occurs through the same route than on Au/CeO_2 but the azoxybenzene and azobenzene formed are hydrogenated very fast on Au/TiO_2, yielding aniline as the sole product (see Scheme 2). We have checked this possibility by reacting azoxybenzene on the Au/TiO_2 catalyst and azobenzene and aniline were formed (see Figure 2). The fact that azobenzene is observed as a primary product and it is accumulated in the reaction media, clearly demonstrates that a very fast hydrogenation of the intermediates azoxybenzene and azobenzene is certainly not the main route to produce aniline on Au/TiO_2.

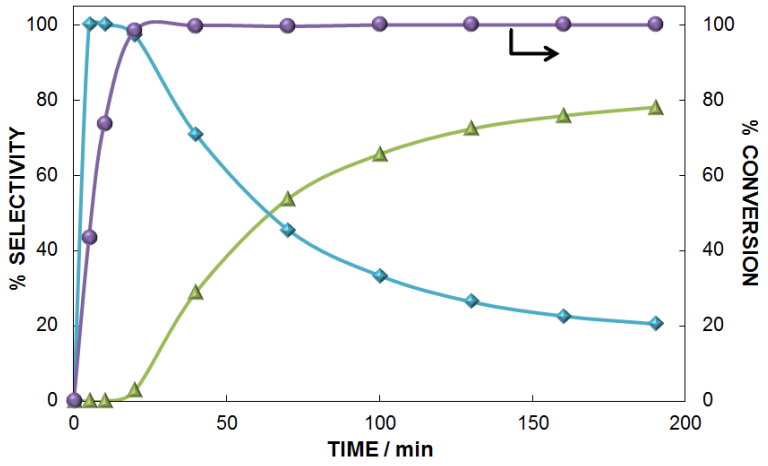

Figure 2. Azoxybenzene reaction profile over Au/TiO_2, 1.5%wt Au load. [Azoxybenzene]= 0.25M in toluene; Au= 1% mol; T= 120 ºC; P_0= 4 bar H_2.

On Au/CeO_2, independently of the hydrogen partial pressure, the consecutive hydrogenation of azobenzene to aniline only occurs when all azoxybenzene has been hydrogenated (Figure S-1 in the supporting information). This result can be explained by assuming that in the case of Au/CeO_2 the adsorption of azoxybenzene is clearly favoured over azobenzene. In other words, the azobenzene would not be able to compete with azoxybenzene for adsorption on the active sites. To test this hypothesis a 50% mixture of azoxybenzene and azobenzene were reacted with Au/CeO_2 and the results in Figure 3 clearly show that no hydrogenation of the azobenzene occurred until all azoxybenzene present in the mixture was consumed. In another experiment azobenzene was reacted on Au/CeO_2 and in a certain moment during the reaction, 40%mol of azoxybenzene was added into the reaction media. Then the formation of aniline immediately stopped, while the concentration of azobenzene started to increase due to the hydrogenation of the azoxybenzene added (Fig. 4).

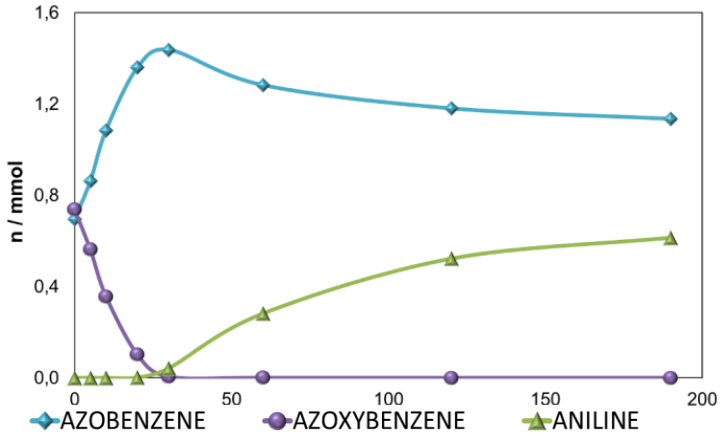

Figure 3. Simultaneous hydrogenation of azobenzene and azoxybenzene over Au/CeO_2, 1.5% wt. gold load. [Azobenzene]= [Azoxybenzene]= 0.25M in toluene; Au= 1% mol; T= 120 ºC; P_0= 4 bar H_2.

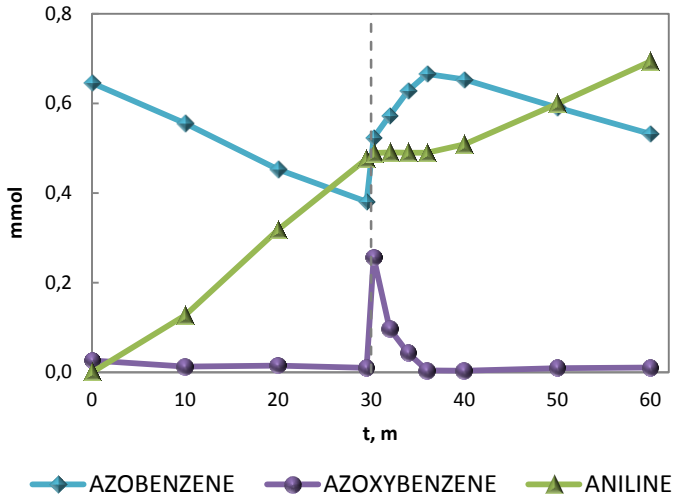

Figure 4. Azobenzene reaction profile over Au/CeO_2 (1.5% wt. gold load), with the addition of 40%mol of azoxybenzene at t= 30min. $[Azobenzene]_0$= 0.25M in toluene; Au= 1% mol; T= 120 ºC; P_0= 4 bar H_2.

From the results presented up to now we can safely conclude that Au/TiO_2 preferentially directs the hydrogenation of nitrosobenzene through the route presented in Scheme 3, while Au/CeO_2 catalyzes the formation of azobenzene through the routes presented in Scheme 4.

The high selectivity to azobenzene obtained with Au/CeO_2 could be explained by the preferential adsorption of azoxybenzene versus azobenzene on the surface of the catalyst, avoiding in this way the hydrogenation of azobenzene into aniline until all azoxybenzene is consumed. Nevertheless there is another possibility to explain the high selectivity of the Au/CeO_2 catalyst to azobenzene, which is a fast reaction of aniline, once formed, with nitrosobenzene to give azobenzene (route b in Scheme 2). We have checked this possibility by reacting nitrosobenzene with isotopically labeled N^{15}-aniline over Au/CeO_2 catalysts (see Figure S-2 in the supporting information). According to the product distribution determined by GC-MS we can conclude that the rate of nitrosobenzene aniline coupling (route b in Scheme 2) is two times faster than the condensation of nitrosobenzene (route a.1 in Scheme 2). From this result, taken into account the product distribution shown in figure 1b for the hydrogenation of nitrobenzene on Au/CeO_2, we can safely assume that the direct hydrogenation of nitrobenzene to nitrosobenzene and aniline (direct route in Scheme 2), should be much slower than the condensation route a.1.

CATALYTIC ROLE OF THE METAL AND THE SUPPORT

One question to be investigated is why the same metal, i.e. gold, follows a different hydrogenation route when supported on TiO_2 or CeO_2. Similar gold particle sizes (2.5-3.5nm) are observed on both Au/CeO_2 and Au/TiO_2 samples, neglecting any influence due to particle size effects. The other possibility we have investigated is that the

support does not act as a simple carrier and could also intervene in the reaction. Then we assumed that perhaps CeO_2 was responsible for the condensation of nitrosobenzene, and, nitrosobenzene and phenylhydroxylamine, since they are the key steps to drive the reaction through the condensation route to form azobenzene (see routes a-1 and a-2 in Scheme 2). To check this hypothesis nitrosobenzene and phenylhydroxylamine have been reacted on TiO_2 and CeO_2 supports, and the reaction was very fast in both cases. Moreover when the blank experiment was done in absence of either TiO_2 or CeO_2 it can be seen that the homogeneous reaction occurs readily and no catalyst is required. It appears then that we cannot associate the catalytic differences to the direct activity of the CeO_2 support.

Nitrosobenzene hydrogenation has also been studied over both Au/TiO_2 and Au/CeO_2 catalysts. Both catalysts direct the reaction by the condensation route to obtain azoxybenzene, azobenzene and aniline, although Au/TiO_2 exhibits a higher activity towards aniline (Figure 5). Taking into account the above results and Scheme 2 it appears that the concentration of nitrosobenzene on the surface of the catalyst and the relative rates of condensation and total hydrogenation can influence the different selectivities shown by Au/CeO_2 and Au/TiO_2. In order to check the validity of the hypothesis, we have undertaken the study of the interaction of reactant and intermediates with the catalyst surface by "in situ" IR spectroscopy on the Au/TiO_2 and Au/CeO_2 catalysts.

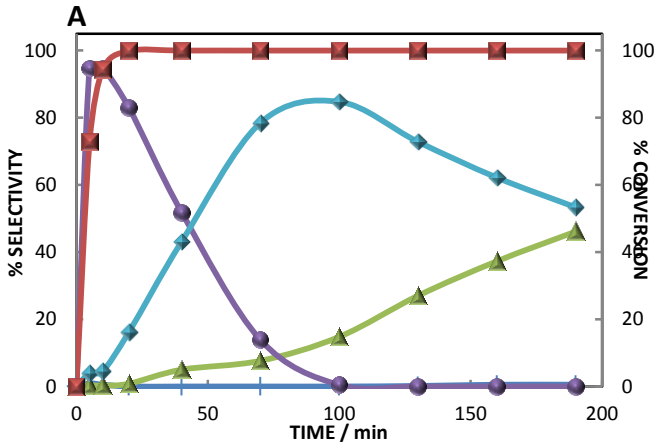

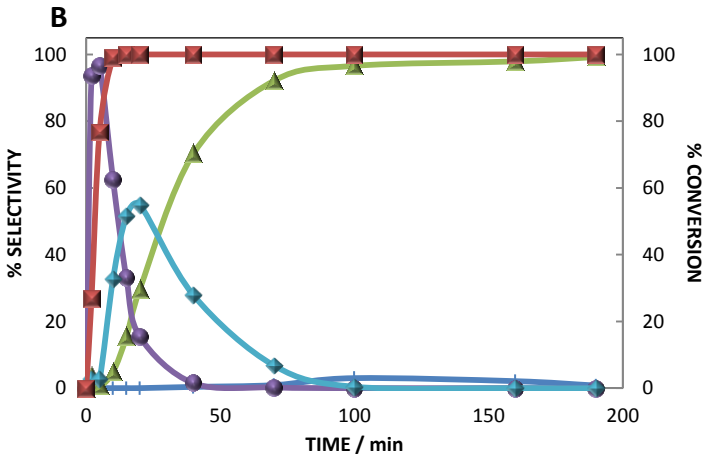

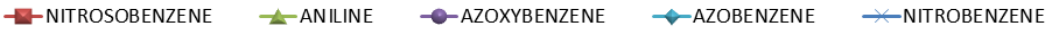

Figure 5. Nitrosobenzene reaction profile over (a) Au/CeO_2, 1.5%wt Au and (b) Au/TiO_2, 1.5%wt Au. [Nitrosobenzene]= 0.25M in toluene; Au= 1% mol; T= 120 ºC; P_0= 4 bar H_2.

IR SPECTROSCOPIC STUDIES

Nitrobenzene adsorbs on both Au/TiO_2 and Au/CeO_2 samples giving two intense IR bands at 1523, 1351 cm^{-1} and 1509, 1343 cm^{-1} respectively, associated to the asymmetric and symmetric stretching vibration of the nitro group. The observed lower frequency shift of the nitro group on the Au/CeO_2 sample can be explained by the higher basicity of the support (Figure 6).

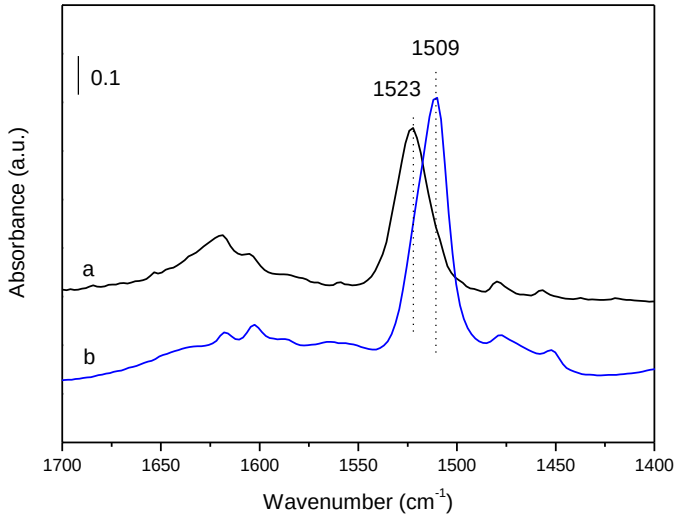

Figure 6. $\nu_{as}(NO_2)$ IR band of nitrobenzene adsorption on Au/TiO_2 (a), and Au/CeO_2 (b)

In opposite, nitrosobenzene adsorbs differently on both catalyst (Figure 7). On Au/TiO_2 nitrosobenzene is found to be coordinated to a surface metal site by a σ-N bonding (characterized by the 1485 cm^{-1} N=O stretching IR band[15, 17]), while on Au/CeO_2, in addition to an interaction of the N=O group by σ-N (IR band at 1485), a σ-O bonding (IR bands at 1520-1508 cm^{-1}) and an interaction of the N=O group with surface oxygen ions (IR band at 1540 cm^{-1}) is observed [17]. The higher basicity of the oxygen ions in the ceria nanoparticles explains the former stabilization mode of nitrosobenzene on the catalysts surface. According to the different interaction mode of nitrosobenzene with the catalyst surface, one may expect a different surface concentration of the intermediate nitrosobenzene on both Au/TiO_2 and Au/CeO_2 catalysts during the hydrogenation of nitrobenzene, which could be responsible of the observed different reaction pathways (illustrated in Scheme 3 and 4). In order to check this hypothesis, first the hydrogenation of nitrosobenzene at different surface concentrations has been

followed by IR spectroscopy and, second, the surface coverage of nitrosobenzene has been in situ followed by IR spectroscopy during the hydrogenation of nitrobenzene.

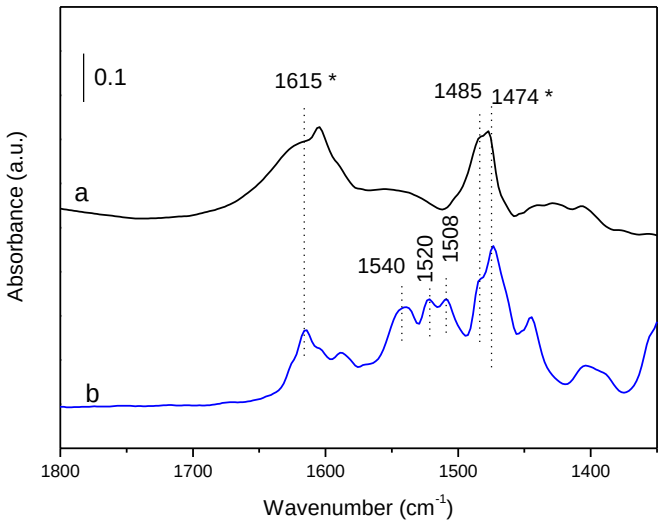

Figure 7. Spectra of nitrosobenzene adsorption on Au/TiO_2 (a) and Au/CeO_2 (b). *IR bands at 1615 and 1474 cm^{-1} are aromatic stretching vibrations (ν8a and 19a).

REACTIVITY OF NITROSO AND NITROBENZENE ON Au/TiO_2 FOLLOWED BY "IN SITU" IR SPECTROSCOPY.

The reactivity of nitrosobenzene on the Au/TiO_2 catalyst has been shown to follow different paths depending on its surface concentration (Figure 8 at low nitrosobenzene coverage and Figures 9a, b at high nitrosobenzene coverage). A fast hydrogenation of nitrosobenzene (IR bands at 1485 cm^{-1} and 1477 cm^{-1}) to phenylhydroxylamine (IR band at 1489 cm^{-1}) is observed at low nitrosobenzene surface coverage (fig.8), followed by further hydrogenation to aniline (IR bands at 1558, 1495, 1280 and 1261 cm^{-1}). At 120 ºC the only observed product on the catalyst surface is aniline. No other bands due to condensation reaction products are observed. At high nitrosobenzene coverage, the scenario is completely different. Azoxybenzene (IR bands at 1483, 1477, 1442, 1319, 1310, 1176, 1115 cm^{-1}) and traces of aniline (IR bands at 1504 and 1600 cm^{-1}) are formed at 25 ºC (fig.9a). At this point, by adding H_2 and increasing the temperature, aniline and azoxybenzene disappear completely followed by azobenzene formation (IR bands at 1484, 1453, 1299 and 1152 cm^{-1}). Aniline disappears due to a fast reaction with nitrosobenzene adsorbed on the catalyst surface, while azoxybenzene is hydrogenated to azobenzene. Increasing the temperature to 120 ºC, further hydrogenation of azobenzene to aniline (IR bands at 1590, 1566, 1492, 1277, 1263, 1155) is observed (Figure 9b).

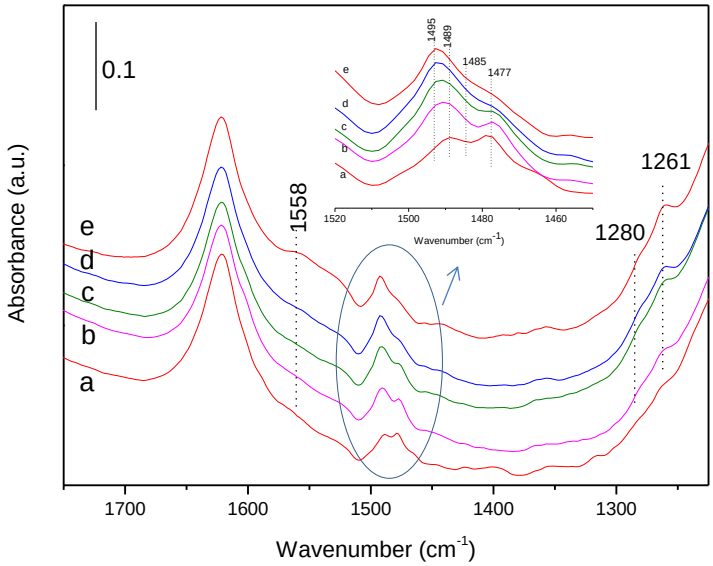

Figure 8. Infrared spectra recorded during the hydrogenation of nitrosobenzene on Au/TiO_2 at: a) 25 ºC, b) 70 ºC, c) 85 ºC, d) 100 ºC and e) 120 ºC. Low nitrosobenzene surface coverage (0.1mbar). Hydrogenation at 8 mbar H_2. Inset: expanded spectra in the 1520-1450 cm^{-1} IR range.

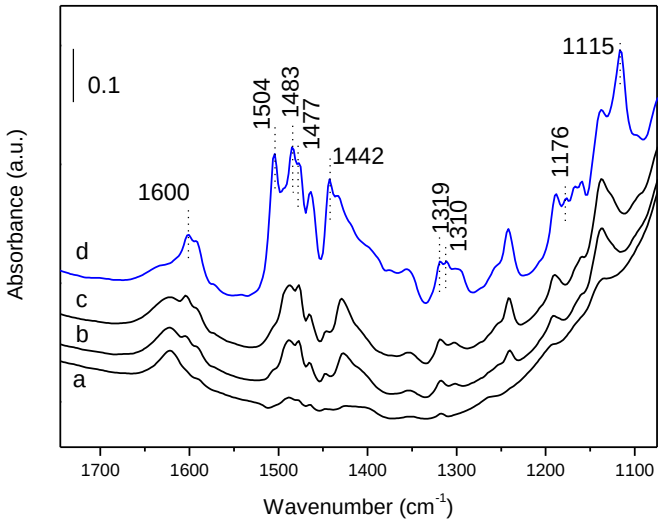

Figure 9a. Spectra of nitrosobenzene adsorption on Au/TiO_2 at increasing coverages a) 0.07 mbar, b) 0.3 mbar, c) 0.5 mbar and d) 1 mbar. Spectra recorded at 25 ºC and in absence of H_2.

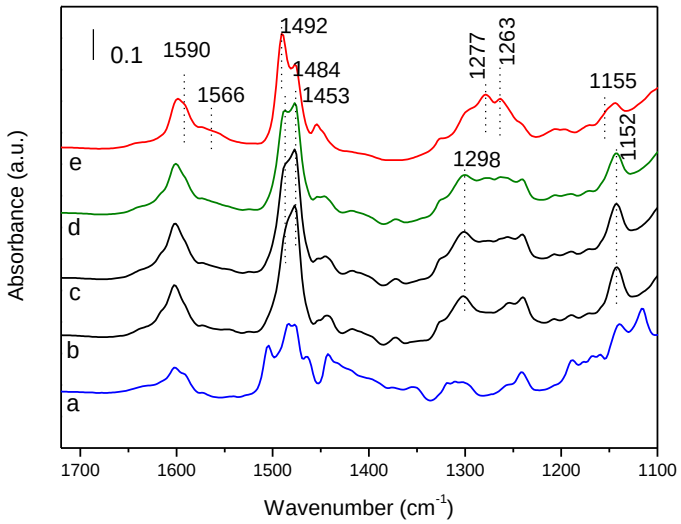

Figure 9b. Infrared spectra recorded during the hydrogenation of nitrosobenzene on Au/TiO_2 at: a) 25 ºC, b) 70 ºC, c) 85 ºC, d) 100 ºC and e) 120 ºC. High nitrosobenzene surface coverage (1mbar). Hydrogenation at 8 mbar H_2.

The results presented up to now, indicate that the concentration of nitrosobenzene on the Au/TiO_2 catalyst surface is decisive in directing the hydrogenation of nitrobenzene through the different paths. From previous macrokinetic data we have concluded that the Au/TiO_2 catalyst directs the hydrogenation of nitrobenzene through the direct hydrogenation path shown in Scheme 3. According to the IR data, this would involve a low surface concentration of the intermediate nitrosobenzene compound on the catalyst surface. In order to check that hypothesis, the hydrogenation of nitrobenzene has been followed by "in situ" IR spectroscopy. Figure 10a shows the IR spectra corresponding to the hydrogenation of nitrobenzene over Au/TiO_2 at different temperatures. Nitrobenzene disappears very fast, monitored by the 1523 cm^{-1} IR band, while new bands at 1475 (due to nitrosobenzene and phenylhydroxylamine ring vibration), 1483 (nitrosobenzene), 1489 (phenylhydroxylamine) and 1495 cm^{-1} (aniline) are formed. Temperature evolution of the reaction products plotted in Figure 10b shows a very low concentration of nitrosobenzene on the catalysts surface. In opposite, the intermediate phenylhydroxylamine surface product concentration is relatively high and stable which, in agreement with previous work[18], indicates the coexistence of a parallel direct reaction pathway from nitrobenzene to phenylhydroxylamine in which nitrosobenzene formation is circumvent. All this contribute to a low surface concentration of nitrosobenzene during the nitrobenzene hydrogenation on Au/TiO_2 minimizing, therefore, the rate for the condensation route a.1.

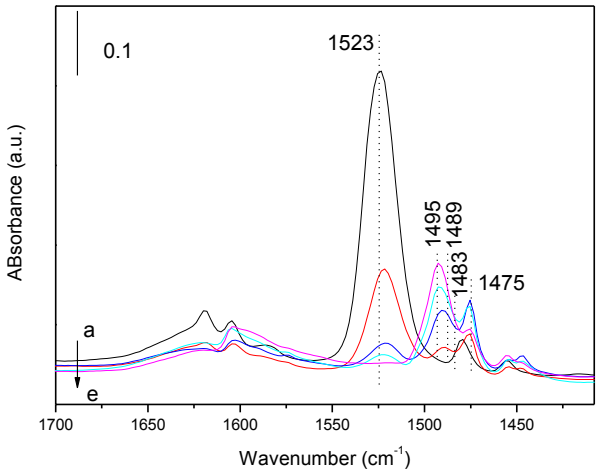

Figure 10a. Infrared spectra recorded during the hydrogenation of nitrobenzene on Au/TiO_2 at: a) 25 ºC, b) 70 ºC, c) 85 ºC, d) 100 ºC and e) 120 ºC. 0.5 mbar nitrobenzene and 8 mbar H_2.

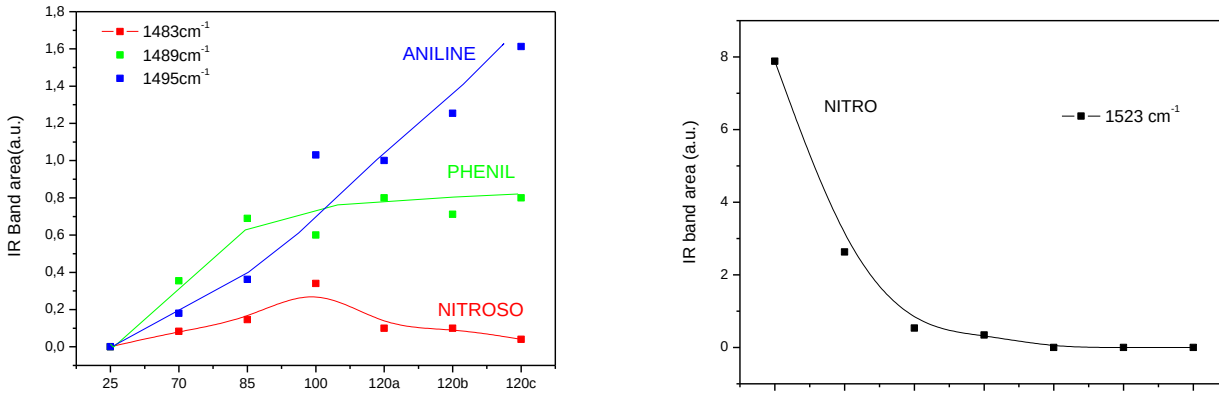

Figure 10b. Evolution of the surface reaction intermediate species in the hydrogenation of nitrobenzene at different temperatures over Au/TiO_2. Areas of the IR bands at 1523 cm^{-1} for nitrobenzene, 1483 cm^{-1} for nitrosobenzene, 1489 cm^{-1} for phenylhydroxylamine and 1495 cm^{-1} for aniline. Temperature nomenclature at 120 ºC: a: 5min, b: 30min and c: 150min.

REACTIVITY OF NITROSO AND NITROBENZENE ON Au/CeO_2 FOLLOWED BY "IN SITU" IR SPECTROSCOPY.

It has been previously shown that nitrosobenzene is stabilized on the Au/CeO_2 catalyst surface by interaction with surface oxygen atoms (see Fig.7). During the hydrogenation of nitrosobenzene on the Au/CeO_2 catalyst, azoxybenzene (characterized by IR bands at 1546, 1372 and 1357cm^{-1}), starts to be formed at 100 ºC independently of the surface coverage. This being further hydrogenated to azobenzene (characterized by the IR band at 1303 and 1563 cm^{-1}). Phenylhydroxylamine intermediate and aniline are not detected (figure 11). Nevertheless, we have to mention that due to the complexity of the IR bands with the Au/CeO_2 sample after nitrosobenzene adsorption, the identification of small amounts of phenylhydroxylamine and aniline is not straightforward. Azoxybenzene and azobenzene formation increases when increasing temperature to 120 ºC. Azobenzene interacts very weakly with the catalyst surface being predominately desorbed to the gas phase (see spectra g in Figure 11 in which reabsorption of azobenzene on the catalyst surface is observed by cooling down the sample). The results show an excellent agreement between micro and macrokinetic data in the sense that the azoxybenzene adsorbs more strongly that the corresponding azobenzene on the catalyst active sites. This, in turns, explains the high selectivity to azobenzene observed with Au/CeO_2 on which the hydrogenation of the azobenzene to aniline does not taken place until all the azoxybenzene has been hydrogenated.

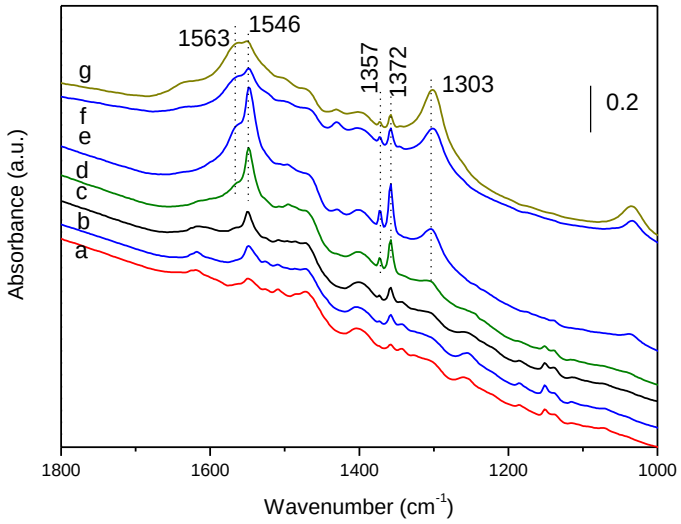

Figure 11. Infrared spectra recorded during the hydrogenation of nitrosobenzene on Au/CeO_2 at: a) 25 ºC, b) 70 ºC, c) 85 ºC, d) 100 ºC, e) 120 ºC 30min, f) 120ºC 150min and g) after cooling down the pellet (re-adsorption of gas phase products). 0.1 mbar nitrosobenzene and 8 mbar H_2.

As we have indicated above, the IR spectra are too complex for assessing the formation of phenylhydroxylamine intermediate specie. Nevertheless the no observation of phenylhydroxylamine on the surface of Au/CeO_2 can also be due to a high reactivity of phenylhydroxylamine, once formed, with nitrosobenzene giving azoxybenzene, in which case phenylhydroxylamine would not be detected in the IR spectra. This possibility has been studied by co-adsorption of both compounds, i.e.

nitrosobenzene and phenylhydroxylamine on Au/CeO_2 (Figure 12). In this case, azoxybenzene formation has been observed even at room temperature in the absence of H_2. Taken into account the fast reactivity of phenylhydroxylamine with nitrosobenzene to give the azoxybenzene, the fact that azoxybenzene starts to be formed at 100 ºC in the hydrogenation of nitrosobenzene, indicates a low hydrogenation rate of nitrosobenzene to phenylhydroxylamine.

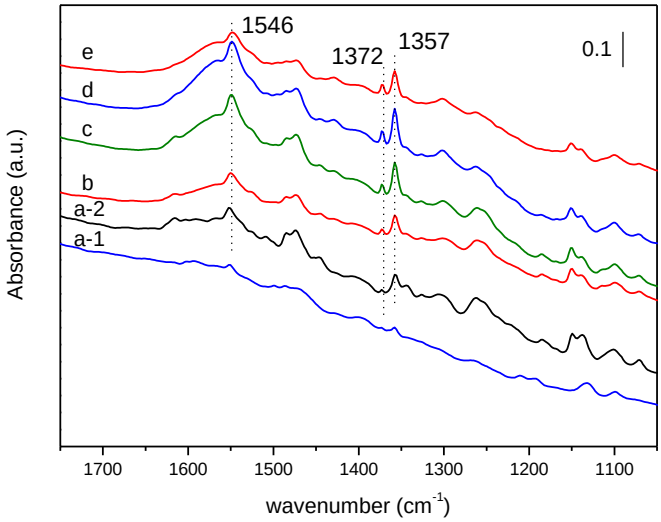

Figure 12. Infrared spectra of phenylhydroxylamine (0.1 mbar) adsorbed on Au/CeO_2 (a-1) followed by nitrosobenzene (0.2 mbar) co-adsorption (a-2) at 25 ºC in absence of H_2. Evolution with temperature at b) 70 ºC, c) 85 ºC, d) 100 ºC and e) 120 ºC. Spectra recorded in absence of H_2.

In order to verify this hypothesis, the hydrogenation of nitrobenzene has been followed on the Au/CeO_2 catalyst by in situ IR spectroscopy. Spectra in Figure 13a shows a slow consumption of nitrobenzene (IR bands at 1509 and 1343cm^{-1}) and the appearance of new broad IR bands, at around 1540, 1491 and 1398 cm^{-1}, which can be assigned to nitrosobenzene. Nitrosobenzene seems to be stabilized on the catalyst surface until 100 ºC in which azoxybenzene starts to be formed (IR bands at 1546, 1372 and 1357cm^{-1}). A further increase of temperature to 120 ºC leads to the formation of azobenzene (IR bands at 1303 and 1566 cm^{-1}) and the disappearance of nitrosobenzene intermediate specie (see Figure 13b for evolution of surface species). Interestingly the IR bands of azobenzene shows a maximum at 21 minutes of reaction at 120 ºC (spectra h in Figure 13a) and then starts to decrease. This is associated to desorption of azobenzene to the gas phase, avoiding in that way a progressive hydrogenation to aniline. In fact, aniline formation has not been detected at 120 ºC neither in the gas phase or adsorbed on the catalyst surface.

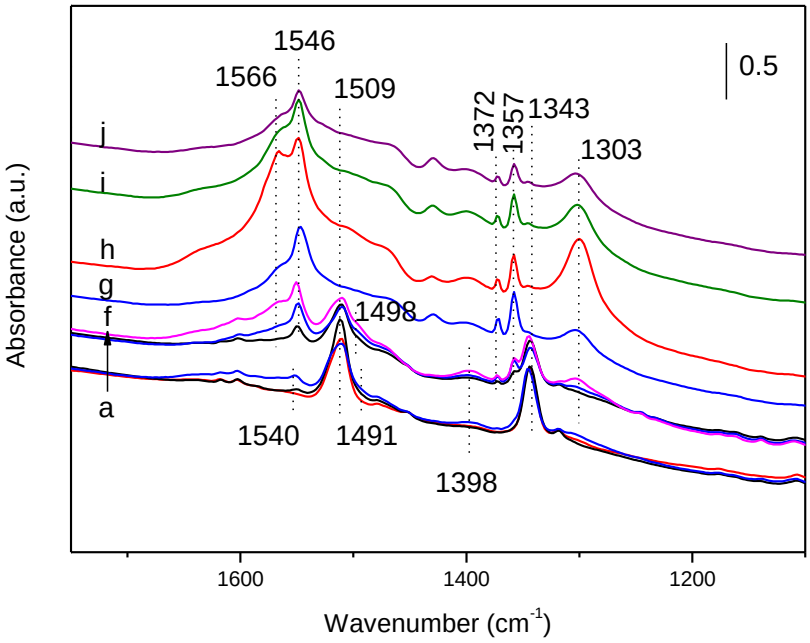

Figure 13a. Infrared spectra recorded during the hydrogenation of nitrobenzene on Au/CeO_2 at: a) 25 ºC, b) 70 ºC, c) 85 ºC, d) 100 ºC 10 minutes, e)100 ºC 30min, f) 120 ºC 7min, g) 120 ºC 17min, h) 120 ºC 21min, i) 120 ºC 26min and j) 120 ºC 46min. 0.5mbar nitrobenzene and 8mbar H_2.

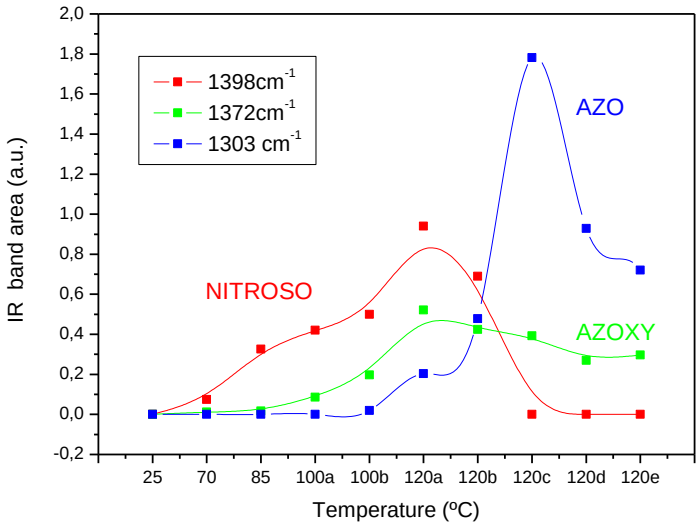

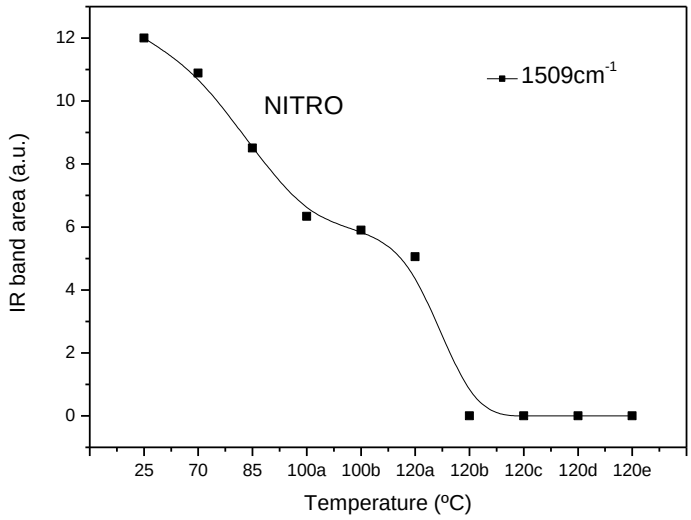

Figure13b. Evolution of the surface reaction intermediate species in the hydrogenation of nitrobenzene at different temperatures on Au/CeO_2. Areas of the IR bands at 1509 cm^{-1} for nitrobenzene, 1398 cm^{-1} for nitrosobenzene, 1372 cm^{-1} for azoxybenzene and 1303 cm^{-1} for azobenzene. Temperature nomenclature at 100 ºC: a) 10min, b) 30min; 120 ºC: a) 7min, b) 17min, c) 21min, d) 26min, e) 46min.

In conclusion, the in situ IR study on Au/CeO_2 proves that a lower reactivity of nitrobenzene and the nitrosobenzene intermediate compound, results in an accumulation of nitrosobenzene on the catalyst surface. Phenylhydroxylamine and aniline have not been detected on the catalysts surface at any temperature which could be related to a fast reactivity of those intermediate species or to a low hydrogenation rate of nitrobenzene to hydroxylamine and aniline. Combining macrokinetic data (product distribution profile in Figure 1b and isotopic exchange data) with IR data we can assume the nitrosobenzene condensation route a.1 as the predominant path during the hydrogenation of nitrobenzene over Au/CeO_2 catalyst.

STABILITY AND REUSABILITY OF THE Au/CeO_2 CATALYST.

To verify if there is leaching of gold from the catalyst, and if the leached species are catalytically active, two identical reactions were initiated in parallel. After 20 minutes the catalyst was removed from one reaction mixture by hot filtration and the reaction was continued while in the other reaction mixture the catalyst was maintained. The results given in Figure S-3, shows that the reaction does not proceed in the absence of the catalyst (see supplementary information).

The catalyst stability was studied by recycling experiments and no loss of conversion and selectivity was observed after four reaction cycles.

CATALYTIC ACTIVITY AND SELECTIVITY OF OTHER NOBLE METALS

The catalytic behavior of Pt and Pd supported on CeO_2 and TiO_2 was also studied, and results given in Figure 14 shows that Pt and Pd on CeO_2 follow the same route than gold, i.e. the reaction route depicted in Scheme 4, though the hydrogenation of the azoxybenzene and azobenzene is much faster than with gold, forming therefore larger amounts of aniline than with the gold catalyst. In the case of Pt and Pd on TiO_2, the products follow exactly the same behavior than with Au/TiO_2, i.e. aniline is the main product. It becomes then evident that a higher hydrogenation activity of the metal, i.e. going from Au to Pt and Pd, results in a loss of selectivity to azobenzene, with the corresponding increase in the formation of aniline.

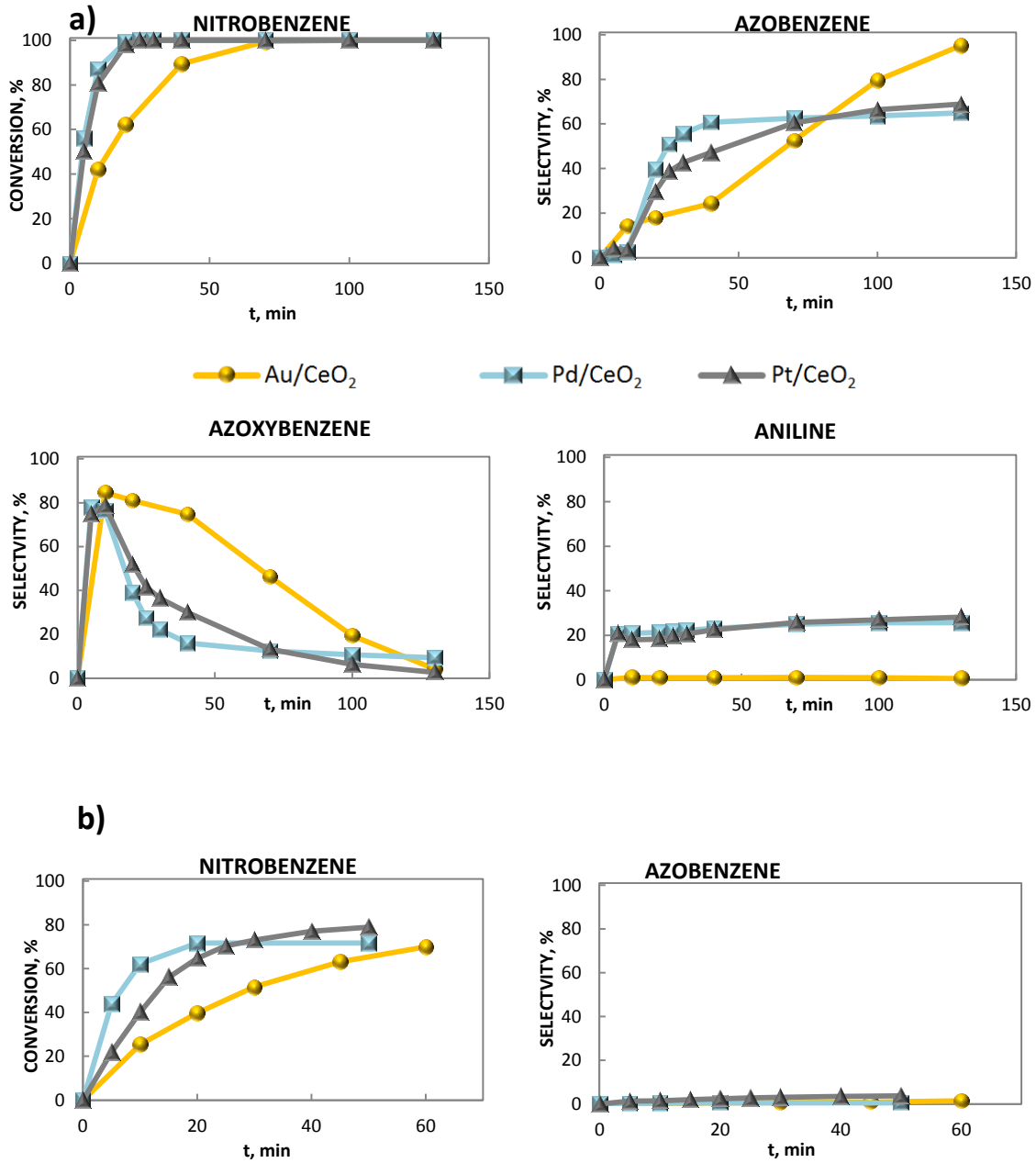

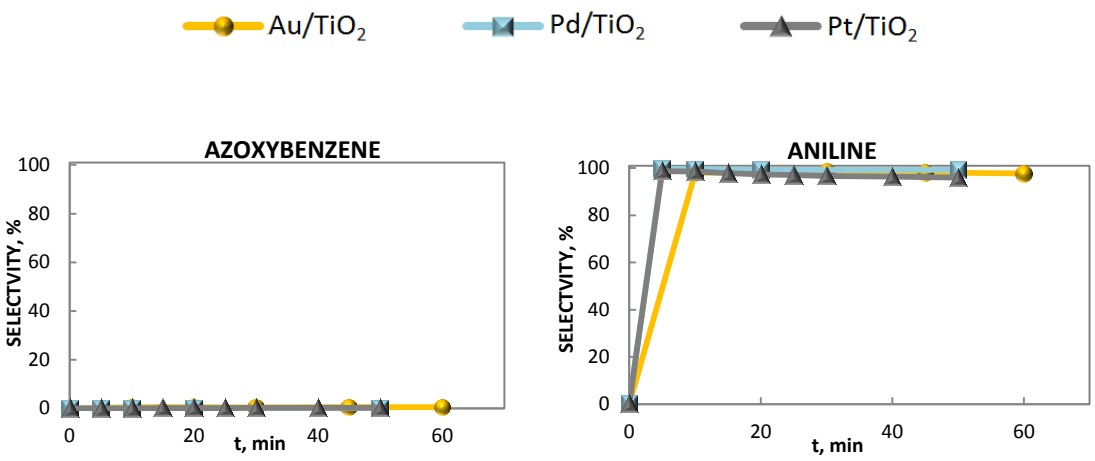

Figure 14. Nitrobenzene reaction profile over a) Au/CeO_2, Pd/CeO_2 and Pt/CeO_2 and b) Au/CeO_2, Pd/CeO_2 and Pt/CeO_2.1.5%wt metal load. [Nitrobenzene]= 0.25M in toluene; metal = 1% mol; T= 120 ºC; P_0= 4 bar H_2.

SCOPE OF THE REACTION AND SYNTHESIS OF ASYMMETRIC AZOCOMPOUNDS

The reaction studied is strongly influenced by the nature of the substituent group (Table 1). Electron donating groups such as $-CH_3$ and $-CHCH_2$ show good selectivity to azocompounds, while electron withdrawing groups such as $–OCH_3$, $-NH_2$ and –OH give the corresponding anilines as main product. Concerning to electron withdrawing groups, –Cl substituent produce a high yield of azocompound while $–COCH_3$ group favors the formation of aniline.

Owing to the high interest of asymmetric azocompounds for the dyes industry, we have reacted mixtures of different aromatic groups, to form the corresponding asymmetric azocompounds. Results in Table 2 show that, unfortunately, Au/CeO_2 exhibits a quite low selectivity to the cross-coupling condensation, while a high selectivity to the desired asymmetric azocompounds is obtained when TiO_2 was used as catalyst (Table 3), this being, as far as we know, the first highly selective alternative solid catalyst for the Mills reaction to produce asymmetric azocompounds.

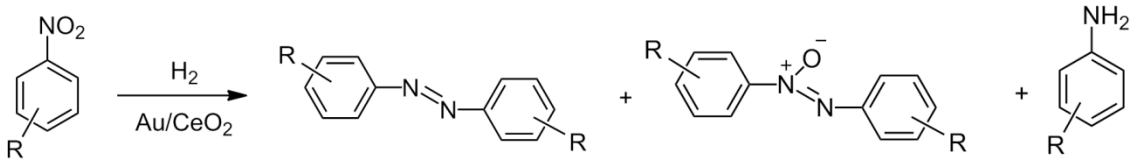

1a-g 2a-g 3a-g 4a-g

R	t (min)	Conversion, %	Selectivity, % 2a-e	3a-e	4a-e
p-CH_3[♦]	130	100	93.0	0.5	6.5
m-$CHCH_2$[♦]	130	100	94.6	0.8	4.6
p-Cl[*]	60	100	95.4	0.5	4.1
p-OCH_3[*]	220	100	4.3	14.1	81.6
p-$COCH_3$[*]	220	100	4.2	28.3	67.5
p-NH_2[†]	250	68	0	0	100
p-OH[†]	250	60	0	0	100

Table 1. Results of the reaction of different substituted nitrocompounds over Au/CeO_2, 1.5%wt Au; [Nitrocompound]= 0.25M ([♦]in toluene, [*]in p-xylene, [†]in diglyme); Au= 1% mol; T= 120 ºC; P_0= 4 bar H_2.

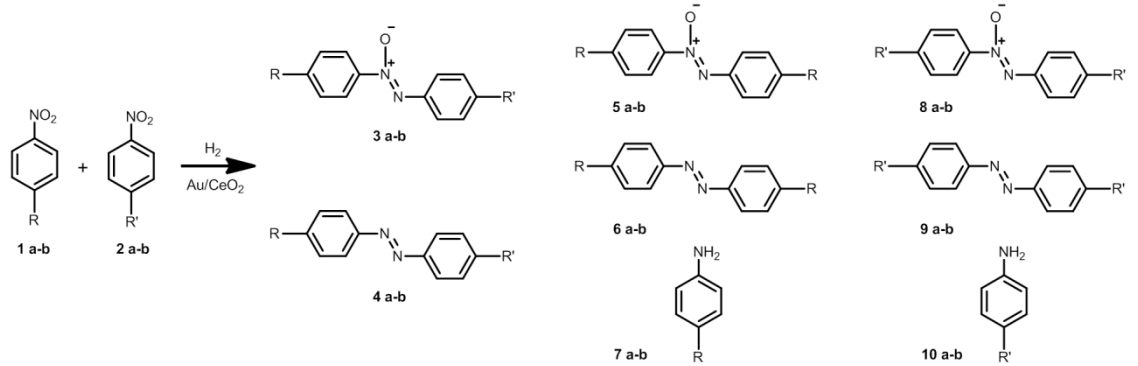

R	R'	t(min)	Conversion, % R	R'	Selectivity[*], % 3a-b	4a-b	5a-b	6a-b	7a-b	8a-b	9a-b	10a-b
H[♦]	CH_3	160	100	100	12.5	34.3	3.6	21.7	2.1	9.6	13.6	2.6
CH_3[†]	$COCH_3$	20	14.2	70.4	15.8	6.1	0.2	1.4	9.6	38.8	4.7	23.4

*At maximum asymmetric azobenzene selectivity.

Table 2. Results of the cross-coupling of different substituted nitrocompounds over Au/CeO_2, 1.5%wt Au; [Nitrocompounds]= 0.25M ([♦]in toluene, [†]in p-xylene); Au= 1% mol; T= 120 ºC; P_0= 4 bar H_2.

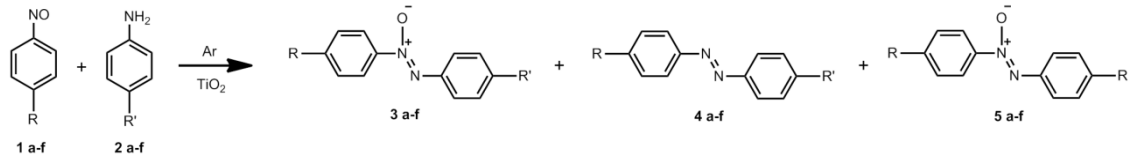

R	R'	t(min)	Conversion, %		Selectivity, %		
			R	R'	3 a-f	4 a-f	5 a-f
H	H	100	100	46	0	93	7
H	CH_3	100	100	47.5	0	94.3	5.7
H	Cl	120	100	49.3	0	94.8	5.2
H	$N(CH_3)_2$	120	100	39	12.1	60.4	27.5
CH_3	H	120	100	45.3	0	88	12
Cl	H	120	100	57.6	0	94.1	4.5

Table 3. Results of the cross-coupling of different substituted nitrosocompounds and anilines over TiO_2. [Nitrosocompound]= 0.125M, [Aniline]= 0.25M in toluene; TiO_2= 1.6 eqv./Nitrosocompound; T= 120 ºC; P= 2 bar Ar.

CONCLUSIONS

Gold supported on nanocrystalline cerium oxide allows the synthesis of symmetric azocompounds from nitrocompounds in a single reduction step with high activity and selectivity. The key steps of the reaction are the surface couplings between adsorbed nitrosocompound, and nitrosocompound with phenylhydroxylamine to form azoxybenzene. The azobenzene adsorption on the catalyst surface is much weaker than the azoxybenzene. Consequently, the non-desired hydrogenation of the azobenzene to the aniline only occurs when the azoxybenzene has been completely hydrogenated. This catalyst shows a high stability and reusability.

Additionally, the reactions between different intermediate compounds reveals the high activity of titanium dioxide for the nitrosobenzene-aniline coupling, which opened an heterogeneous way to obtain asymmetric azocompounds with high selectivity.

EXPERIMENTAL SECTION

All the reactives used in this study, except the substituted nitrosocompounds, are commercially available from Sigma-Aldrich with purities higher than 95%, and were used without further purification. n-dodecane was used as internal standard to determine conversions and selectivities by GC.

All the nitrosocompounds was synthesized according to Lutz and Lytton[19] and purified by steam distillation and/or sublimation.

Nanocrystalline ceria was prepared by adding an aqueous ammonia solution (1.12L, 0.8M) to 375 mL of a $Ce(NO_3)_4$ solution (0.8M) at ambient temperature under vigorous stirring. The milky slurry was transferred to a polyethylene terephthalate vessel and heated at 373 K for 24 h. The resulting yellow precipitate was filtered and dried under vacuum overnight. The cerium oxide synthesized has, owing to the small size of the nanoparticles, a very large BET surface area, 115 m^2/g.

Catalysts

Au/CeO_2: First, a 30 wt % $HAuCl_4 \bullet 3H_2O$ solution was prepared in 15 wt% HCl in H_2O. The dissolution of $HAuCl_x$ in HCl promotes the transformation of $AuCl_x$ to $Au(OH)_x$ markedly and improves overall reproducibility of the method. The appropriate amount of $HAuCl_4$/HCl solution to obtain a nominal loading of 1.5 wt % Au was dissolved in approximately 400 mL of H_2O and heated up to 70 °C and maintained for the duration of the preparation. The pH of the solution was adjusted near to pH 5 with 0.2M NaOH and 3000 mg of CeO_2 was added under vigorous stirring. Then, the pH of the slurry was readjusted at pH 8.0. After 30 min, the solution was cooled in an ice bath and centrifuged three times. After each centrifuge run, the supernatant was replaced with clean deionized H_2O and the catalyst redispersed with agitation. Finally, the catalyst was filtered under vacuum until dry, further dried overnight at 120 °C in flowing dry air, and then calcined at 400 °C.

Au/TiO_2: The previous procedure was also used for this catalyst but the deposition stage was carried at pH 7.0. Additional to the calcination stage, this catalyst was reduced in pure H_2 flow at 400 ºC for 3 hours.

Pt/CeO_2 and Pd/CeO_2: The appropriates amounts of precursors $Pt(NH_2)_4(OH)_2$, $Pd(NO_3)_2$, respectively) were dissolved in deionized H_2O and 1000 mg of CeO_2 was incipient impregnated in each case. Then the catalysts were dried at 100 ºC overnight and reduced in pure H_2 flow at 400 ºC for 3 hours.

The gold content measurements were performed using a Panalytical Minipal 4 EDXRF spectrometer equipped with a rhodium anode tube operated at 30kV and 300mA, using an Ag filter in air atmosphere. The metal content of the other catalysts were determined by chemical analysis, after dissolution of the solids in a HCl/HNO_3/HF solution, in a Varian 715-ES inductively coupled plasma optical emission spectrometer.

Kinetic measurements

Catalytic experiments were performed in 10 mL reinforced glass reactors. In a typical experiment 3 mL of the reactives solution and the adequate amount of gold catalyst were added to the glass reactors. The reactors were sealed, purge with hydrogen four times, loaded at the adequate pressure and deeply introduced into a silicone bath preheated at 120 ºC. During the experiment, the reaction mixtures were magnetically stirred at 1000 rpm. The course of the reaction was monitored by analyzing aliquots taken at different times during the reaction. The reaction samples were analyzed by GC/MS methods for identification purposes, using an Agilent 6890N chromatograph coupled with an Agilent 5973 Mass selective detector. The chromatograph was

equipped with a capillary column (30m length; 0.25mm I.D.; 0.25µm film) with 5% phenyl-methylpolisiloxane as stationary phase. In the isotopic experiment the relation between azobenzene isotopes was calculated using the relative intensities of the m/z signals at 182 (azobenzene) and 183 (azobenzene ^{15}N). For quantification purposes, an Agilent 7890A chromatograph equipped with FID detector and a capillary column (30m length; 0.32mm I.D.; 0.25µm film) with 5%-phenyl-methylpolisiloxane as stationary phase was used.

Phenylhydroxylamine conversion was analyzed in a Varian Pro-Star HPLC system with a U.V. photodiode array detector adjusted at 254nm. Separation was carried at ambient temperature using an Eclipse Plus C-18 (5mm, 150x4.6 mm i.d.; Agilent) column. The mobile phase consisted of acetonitrile–water (85:15 v/v from 0 to 3 min. and 75:25 v/v from 3 to 15 min) at a flow rate of 1.0 ml min^{-1}. The calculations concerning the quantitative analysis were performed with external standardization by measurement of peak areas.

IR study

In situ FTIR experiments have been performed with a Nexus 8700 FTIR spectrometer using a DTGS detector and acquiring at 4 cm^{-1} resolution. A quartz IR cell allowing in situ treatments in controlled atmospheres and temperatures from 25 ºC to 600 ºC has been connected to a vacuum system with gas dosing facility. Prior to the adsorption experiments the Au/CeO_2 sample were treated at 350 ºC in oxygen flow (20 $ml \cdot min^{-1}$) for 2 h followed by evacuation at 10^{-5} mbar at the same temperature for 1h, in order to remove adsorbed carbonate species. The Au/TiO_2 sample was activated at 350 ºC in vacuum (10^{-5}mbar) for 1h. After activation the samples were cooled down to 25 ºC under dynamic vacuum conditions followed by reactant adsorption experiments at defined pressure (0.1-8.0 mbar). IR spectra were recorded after each dosage. IR spectra of pure compounds (aniline (Aldrich 99%), nitrobenzene (Aldrich 99%), nitrosobenzene (Aldrich, 97%), phenylhydroxylamine (Aldrich, 97%), azoxybenzene (Alfa Aesar, 98%) and azobenzene (Aldrich, 98%),) has been recorded on IR transparent germanium disc (Spectra included in the supporting information, Figure S-4). The integration procedure used to determine the surface concentration of reaction intermediate species has been done by using the ORIGIN 7.0 software. Since extinction coefficients are not known peak areas cannot be compared in a quantitative mode.

Acknowledgements

The authors wish to acknowledge the financial support from the Spanish Ministries of Education and Science and Economy and Competitiveness under the project Consolider-Ingenio 2010 (CSD2009-00050 “Development of more efficient catalysts for the design of sustainable chemical processes and clean energy production”) and the Severo Ochoa program (SEV-2012-0267), respectively. D.C. thanks the Spanish MEC for postgraduate scholarship, project MAT2006-14274-C02-01.

Keywords

Azocompounds – Nitroaromatics reduction – Heterogeneous catalysts – Gold catalysts – Hydrogenation.

References

[1] E. Merino, *Chemical Society Reviews* **2011**, *40*, 3835-3853.

[2] A. T. Peters, H. S. Free, *Colour chemistry : the design and synthesis of organic dyes and pigments*, Elsevier applied science, **1991**.

[3] R. J. Chudgar, in *Kirk-Othmer. Encyclopedia of chemical technology, Vol. 3*, 4 th. ed. (Ed.: M. Howe-Grant), John Wiley & Sons., **1992**.

[4] W. J. Sandborn, *Am J Gastroenterology* **2002**, *97*, 2939-2941.

[5] H. Zollinger, *Color chemistry : syntheses, properties, and applications of organic dyes and pigments*, 3rd ed., Wiley-VCH, **2003**.

[6] M. Wang, K. Funabiki, M. Matsui, *Dyes and Pigments* **2003**, *57*, 77-86.

[7] C. Mills, *Journal of the Chemical Society, Transactions* **1895**, *67*, 925-933.

[8] E. Buncel, *Accounts of Chemical Research* **1975**, *8*, 132-139.

[9] a) R. F. Nystrom, W. G. Brown, *Journal of the American Chemical Society* **1948**, *70*, 3738-3740; b) W. Tadros, M. S. Ishak, E. Bassili, *Journal of the Chemical Society (Resumed)* **1959**, 627-630; c) R. O. Hutchins, D. W. Lamson, L. Rua, C. Milewski, B. Maryanoff, *The Journal of Organic Chemistry* **1971**, *36*, 803-806; d) Y. Moglie, C. Vitale, G. Radivoy, *Tetrahedron Letters* **2008**, *49*, 1828-1831.

[10] A. Grirrane, A. Corma, H. García, *Science* **2008**, *322*, 1661-1664.

[11] H. Zhu, X. Ke, X. Yang, S. Sarina, H. Liu, *Angewandte Chemie International Edition* **2010**, *49*, 9657-9661.

[12] L. Hu, X. Cao, L. Chen, J. Zheng, J. Lu, X. Sun, H. Gu, *Chemical Communications* **2012**, *48*, 3445-3447.

[13] M. Makosch, J. Sá, C. Kartusch, G. Richner, J. A. van Bokhoven, K. Hungerbühler, *ChemCatChem* **2012**, *4*, 59-63.

[14] F. Haber, *Z. Elektrochem* **1898**, *4*, 506.

[15] G. Richner, J. A. van Bokhoven, Y.-M. Neuhold, M. Makosch, K. Hungerbuhler, *Physical Chemistry Chemical Physics* **2011**, *13*, 12463-12471

[16] P. Zuman, B. Shah, *Chemical Reviews* **1994**, *94*, 1621-1641.

[17] S. Meijers, V. Ponec, *Journal of Catalysis* **1996**, *160*, 1-9.

[18] A. Corma, P. Concepción, P. Serna, *Angewandte Chemie* **2007**, *119*, 7404-7407.

[19] R. E. Lutz, M. R. Lytton, *The Journal of Organic Chemistry* **1937**, *02*, 68-75.